Transforming Medicine with Deep Learning: Applications in Disease Detection using Medical Images

Iqra Nissar[1], Aqib Nazir Mir[1], Asif Hussain[2], Waseem Ahmed Mir[3], Mohammad Kashif[1]

[1]Department of Computer Engineering, Jamia Millia Islamia, New Delhi, India
[2] Sri Sai Group of Institutions, Punjab, India
[3] GH Raisoni College of Engineering and Management, Wagholi Pune, India

Abstract
In recent times, data analytics in health informatics have become increasingly important due to the tremendous increase in multimodal data. Deep learning has emerged as a powerful tool in medical imaging, influencing many facets of the diagnostic and treatment processes. Recent developments in artificial intelligence, particularly in the field of deep learning, are assisting in the detection, categorization, and quantification of patterns in medical images. One of the most important developments is the ability to use hierarchical feature representations acquired entirely from data rather than features developed by hand using domain-specific expertise. Deep learning is becoming the state-of-the-art, resulting in improved outcomes across a range of medical applications. Within the realm of medical imaging, deep learning has ushered in a new era of remarkable advancements in disease detection. In this chapter, the remarkable applications of deep learning in disease detection are explored across diverse fields like neurology, cancer detection, ophthalmology, all through the lens of medical imaging. The transformative power of deep learning algorithms emerges as they navigate the intricate landscapes of medical imaging, unveiling hidden patterns and anomalies. From unraveling neurological disorders to cancer detection, these intelligent systems reshape the landscape of medicine, offering hope and healing with every pixel they analyze.

1. Introduction

Deep learning (DL) has made a significant impact across a wide range of scientific field [1] . It has resulted in notable advancements in speech recognition [2] and image recognition [3], leading to substantial improvements. In addition to these, deep learning has found its applications in various other fields which include natural language processing, robotics, healthcare, finance, generative models, recommendation systems, drug discovery and many more. With the significant advancement in image acquisition technology, the amount of medical image data has grown exponentially, presenting both challenges and opportunities for analysis. Manual analysis by medical experts is subjective, time-consuming, and prone to errors. To address this, machine learning techniques have emerged as a potential solution, but traditional methods fall short when dealing with complex problems. The combination of high-performance computing and deep learning holds great promise in effectively handling large medical image datasets, automating diagnosis, and extracting meaningful features. Deep learning not only aids in disease detection but also enables predictive modeling and provides actionable insights for physicians, improving efficiency and accuracy in diagnosis.

Undoubtedly, this technology finds significant relevance in medical imaging. Numerous introductions to the subject can be discovered in the literature, spanning from concise tutorials and reviews [4–7], interactive Jupyter notebooks, to comprehensive books [8,9]. Each of these resources serves a unique purpose and offers diverse perspectives on this rapidly evolving and dynamic topic. Medical imaging techniques, including computed tomography (CT), magnetic resonance imaging (MRI), positron emission tomography (PET), mammography, ultrasound, and X-ray, play a vital role in the early detection, diagnosis, and treatment of diseases. These techniques provide detailed images of internal structures, allowing healthcare professionals to identify abnormalities, assess disease progression, and develop appropriate treatment plans. By utilizing deep learning and imaging modalities, medical imaging enables early detection of diseases. These imaging techniques aid in accurate diagnosis, guiding physicians in making informed decisions for timely intervention and effective treatment, ultimately improving patient outcomes and prognosis.

This chapter offers an extensive analysis of DL based algorithms as they have been applied to the various problems of medical image processing. The objective of this chapter is to discuss the fundamental principles of deep learning and explore the latest and most advanced techniques for its application in medical image processing and analysis.

2. Deep Learning over Machine Learning

DL is a subset of machine learning that has gained prominence and preference over traditional machine learning approaches in certain domains, including medical imaging. There are several reasons why deep learning is often favored over conventional machine learning methods:

Representation Learning: Deep learning algorithms can automatically learn hierarchical representations of data. Unlike traditional machine learning methods that require manual feature engineering, deep learning algorithms can learn complex features directly from raw data. This ability to automatically learn hierarchical representations enables deep learning models to capture intricate patterns and relationships within the data, which can be especially beneficial in complex tasks like image analysis.

Scalability: Deep learning algorithms are highly scalable. They can handle large and high-dimensional datasets, making them well-suited for medical imaging, which often involves massive amounts of data. Deep learning models can effectively utilize powerful computing resources, such as GPUs to process and analyze large volumes of medical images efficiently.

Performance: Deep learning models have demonstrated remarkable performance in various domains, including medical imaging. They have achieved state-of-the-art results in tasks such as image classification, object detection, and segmentation. Deep learning algorithms can often outperform traditional machine learning approaches when provided with abundant labeled data for training as indicated in figure 1. This increased performance can lead to improved accuracy in disease detection, diagnosis, and treatment planning.

End-to-End Learning: Deep learning allows for end-to-end learning, where the model learns to directly map input data to desired outputs. This eliminates the need for manual intermediate steps and simplifies the overall pipeline. In medical imaging, deep learning models can take raw image data as input and directly generate predictions or assist in decision-making without relying on explicitly engineered features or pre-processing steps.

Adaptability: Deep learning models are highly adaptable and can learn from diverse types of data. They can handle different imaging modalities, such as CT, MRI, PET, and ultrasound, by effectively learning from the specific characteristics of each modality. Additionally, deep learning models can learn from large, heterogeneous datasets, incorporating a wide range of patient demographics, disease subtypes, and imaging variations, which can contribute to improved generalization and robustness.

While deep learning offers numerous advantages, it is important to note that traditional machine learning methods still have their own merits and may be more suitable for certain tasks with limited data or interpretability requirements. The choice between deep learning and traditional machine learning depends on the specific problem, available data, computational resources, and interpretability needs.

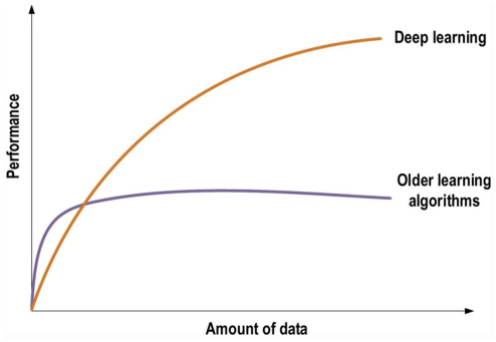

Figure 1. Performance of deep learning with data.

3. Deep Learning Architectures

Deep learning architectures are complex neural network structures that consist of multiple layers of interconnected artificial neurons. These architectures are designed to learn and extract meaningful representations from raw input data, enabling them to solve complex problems. The taxonomy of commonly used deep learning architectures is illustrated in Figure 2. Table 1 entails the pros and cons of various DL architectures.

3.1 Convolutional Neural Networks (CNNs)

CNNs are extensively utilized in computer vision applications, particularly for image analysis. CNNs consist of several essential layers, including convolutional layers, pooling layers, and fully connected layers [10]. The central concept underlying CNNs revolves around the utilization of convolutional layers, which conduct localized receptive field operations, enabling the network to capture spatial patterns and features within images [11]. These layers employ filters or kernels to scan the input data for creating feature maps which emphasize specific patterns or objects. Pooling layers reduce the spatial dimensions of the feature maps while preserving the most pertinent information. Fully connected layers, also referred to as dense layers, play a vital role in making ultimate predictions based on the acquired features.

Table 1. Pros and Cons of different DL architectures.

Network Type	*Network Details*	*Pros*	*Cons*
Convolutional Neural Network (CNN)	It is a specialized type of DNN designed to effectively process grid-like data, such as images or time series, by using convolutional layers that capture local patterns and hierarchies of features.	1.Effective Feature Learning 2.Translation Invariance 3.Parameter Sharing and Efficiency	1. Lack of Global Context 2. Large Memory and Computation Requirements 3. Limited Data Efficiency
Recurrent Neural Network (RNN)	It is a type of NN designed for sequential data processing, where the output of a previous step is fed as input to the current step. This architecture enables RNN's to capture temporal dependencies and effectively model time series, natural language processing, and other sequential tasks.	1.Sequential Modeling 2.Variable-Length Inputs 3.Temporal Dynamics	1.Vanishing and Exploding Gradients 2.Sequential Computation 3.Difficulty with Long Sequences
Auto-Encoder (AE)	It is a type of neural network architecture that is trained to reconstruct its input data at the output layer, effectively learning a compressed representation of the data in the hidden layers.	1.Dimensionality Reduction and Feature Learning 2. Data Compression and Denoising 3.Generative Modeling	1.Overfitting and Reconstruction Bias 2.Lack of Interpretable Latent Space 3.Difficulty Scaling to Large Datasets
Generative Adversarial Networks (GANs)	This framework comprises two neural networks: a generator and a discriminator, engaged in a competitive process. The generator's objective is to acquire the ability to produce synthetic data that closely resembles real data, while the discriminator is tasked with distinguishing between authentic and counterfeit data. This competition between the two networks ultimately results in the creation of synthetic samples that are exceptionally realistic and diverse.	1.High-Quality Data Generation 2.Creative and Diverse Outputs 3.Adversarial Training	1.Expensive Computational Requirements 2.Training Instability 3.Mode Dropping and Evaluation
Transformer	The Transformer is a NN architecture that utilizes self-attention mechanisms to capture global dependencies in sequential data, making it highly effective in tasks such as machine translation, text generation and natural language understanding. It eliminates the need for recurrent connections, enabling parallelization and improving performance.	1.Capturing Long-Range Dependencies 2.Parallelization and Scalability 3. Interpretability and Visualization	1.High Memory Requirements 2.Lack of Sequential Order 3.Limited Efficiency for Small-Scale Tasks

3.2 Recurrent Neural Networks (RNNs)

RNNs are specifically designed for processing data that unfolds sequentially, such as time-series information. Unlike feedforward networks, RNNs incorporate recurrent connections, allowing information not only to flow from input to output but also to persist across different time steps [12]. This distinctive architecture empowers RNNs to capture temporal relationships and retain a memory of previous inputs. RNNs are composed of recurrent units, including the basic RNN unit, Long Short-Term Memory (LSTM), and Gated Recurrent Unit (GRU). These

are RNN variants which effectively address issues like the vanishing gradient problem, and makes them highly suited for capturing long-term dependencies. RNNs find extensive applications in various domains, including NLP, sentiment analysis, speech recognition, and time-series prediction.

3.3 Autoencoders

Autoencoders represent neural networks designed to learn a condensed representation known as the latent space and are subsequently trained to reconstruct input data. This architecture comprises an encoder network responsible for mapping input data into the latent space and a decoder network that performs the task of reconstructing the original input based on this latent representation [13]. Autoencoders are classified as unsupervised learning models capable of extracting meaningful features from input data. They find application in various tasks, including data compression, anomaly detection, noise reduction, and dimensionality reduction.

3.4 Transformers

The Transformer architecture has gained prominence in natural language processing tasks. Transformers are designed to capture global dependencies between input and output sequences without the need for recurrent connections. They use a self-attention mechanism to compute attention scores between all positions in the input sequence, allowing the model to focus on relevant information and establish long-range dependencies. Transformers are composed of two essential components: an encoder and a decoder. In this architecture, the encoder handles the input sequence, while the decoder is responsible for generating the output sequence. Transformers have demonstrated remarkable performance, reaching the forefront in tasks such as machine translation, language comprehension, and text generation.

3.5 Generative Adversarial Networks (GANs)

GANs are structured with two key neural networks: a generator and a discriminator network. In the training of GANs, the generator network's goal is to create synthetic data samples, while the discriminator network is focused on differentiating between genuine and counterfeit data. The generator network improves its ability to produce more authentic samples by incorporating feedback from the discriminator network. The discriminator network, in turn, improves its ability to discriminate between real and fake data by analyzing both real and generated samples. GANs have shown impressive results in image synthesis, style transfer, data augmentation, and generating realistic synthetic data.

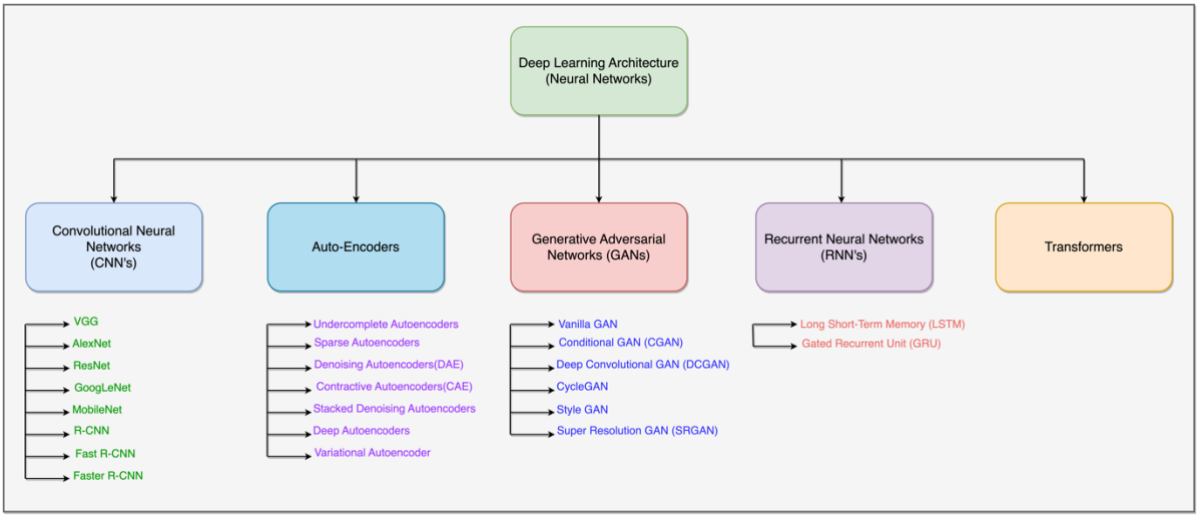

Figure 2 . Taxonomy of variants of deep learning architectures.

4. Deep Learning in Disease Diagnosis

In this section, a substantiated overview is presented, highlighting the wide-ranging applications of deep learning in the context of diagnosing various diseases. It offers an exhaustive analysis of how deep learning techniques have been utilized to address a spectrum of healthcare challenges. The exploration delves into how these methodologies are applied to interpret medical images, predict disease outcomes, and integrate disparate data sources. The review also highlights the significant role that deep learning plays in enhancing early detection, aiding medical professionals in radiology and pathology.

4.1. Neurological Disorders

Neurodegenerative diseases include Alzheimer's and Parkinson's pose serious threats to the elderly population, lacking effective cures. In recent years, the potential of DNNs in medical image analysis and diagnostics has gained traction, and this study is based on the application in detecting Alzheimer's and Parkinson's diseases. The research outlines the pertinent medical examinations for these ailments and delves into various DL models, discussing their frameworks and applications.

Alzheimer's disease (AD)

In the context of exploring biomarkers and intelligently classifying AD using structural MRI, a novel DL model called "modified 3D EfficientNet" is introduced in [14]. This model incorporates the 3D MBConv block, which comprises depthwise convolution and a squeeze-and-excitation module. The results show that the proposed model achieves impressive classification accuracies, specifically reaching 95.00% for NC versus AD, 80.00% for NC versus all MCI, 86.67% for NC versus pMCI, and 83.33% for sMCI versus pMCI comparisons. These results demonstrate the model's effectiveness in detecting early Alzheimer's disease and high-risk mild cognitive impairment, surpassing the performance of traditional networks and existing methods in AD detection and prediction.

In the research detailed in [15], an examination was conducted using a compact MRI image dataset to evaluate the effectiveness of CNN-based classification. A convolutional neural network with a streamlined convolutional layer design was created to identify AD in medical image patches. The results demonstrate that the proposed model achieved an impressive accuracy rate of 98%, surpassing the performance of conventional SVM, NB, and CNN models.

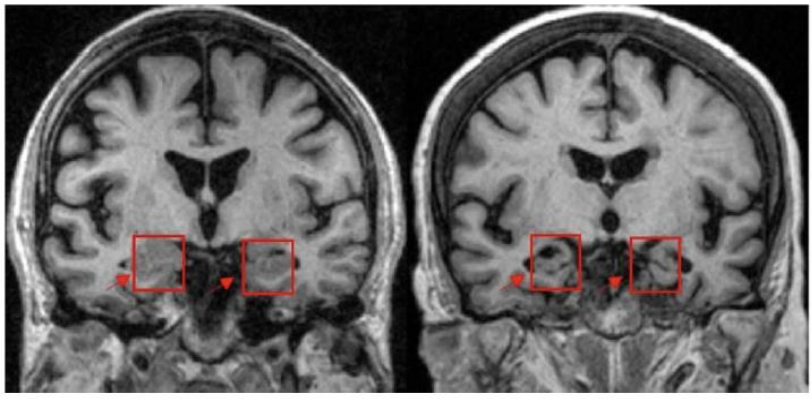

Figure 3. A coronal T1-weighted MRI scan comparison between a patient with Alzheimer's disease (AD) on the right, exhibiting hippocampal atrophy and a healthy individual on the left, featuring an intact hippocampus [16].

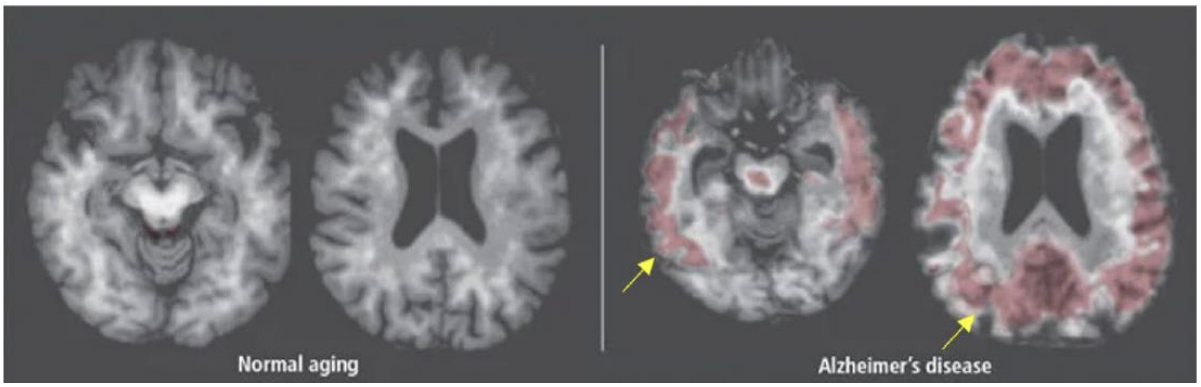

Figure 4. A PET scan contrast, with the left side representing a normal individual and the right side showcasing an Alzheimer's patient. The PET scan highlights the presence of amyloid deposits through the PiB compound [17].

In [18], a novel DL algorithm was introduced for the rapid and automated diagnosis of AD using MRI images. This method incorporates 2D CNN models, dynamic medical images, and structural reparameterization, resulting in an impressive AUC of 0.9849 and accuracy of 0.9625. To capture slice-to-slice variations in MRI images, a temporal pooling technique is employed, while structural reparameterization enhances pre-existing network architectures without introducing additional evaluation-time computational costs. This innovative approach not only reduces diagnosis time but also achieves higher levels of accuracy. Figures 3 and 4 depict coronal T1-weighted MRI and PET scans of a healthy individual and an Alzheimer's patient.

In [19], an assessment was conducted on an advanced and interpretable network algorithm called TabNet. The study aimed to compare the performance of TabNet with that of XGBoost, a commonly employed classifier. Brain segmentation was carried out using commercially approved software, and both algorithms were trained using either volume data or radiomics features. Results showed similar diagnostic performances for AD and MCI groups, with TabNet showing an AUC of 0.951 for volume features and XGBoost showing similar performance in MCI. The other notable contributions for the AD detection is tabulated in Table 2.

Parkinson's disease

In [20], a novel pipeline based on deep learning was introduced for the automatic diagnosis of PD using Quantitative Susceptibility Mapping (QSM) and T1-weighted images. This pipeline incorporates a CNN model along with an SE-ResNeXt50 model. The model effectively performed brain nuclei segmentation and achieved impressive AUCs of 0.901 and 0.845 when tested on independent cohorts. To identify the nuclei contributing to Parkinson's disease diagnosis at the patient level, Gradient-weighted Class Activation Mapping (Grad-CAM) heatmaps were used. Figure 5 provides a visual representation of imaging findings derived from MRI studies and nuclear imaging.

Table 2. Summary of different deep learning approaches for the Alzheimer's disease detection.

Author	Image Modality	Models Employed	Results
Mehmood et al.[21]	MRI	VGG – 16	Accuracy: 99%
Basher et al.[22]	sMRI	CNN and DNN	*AD vs NC (based on right hippocampal volume)* Accuracy: 94.02% *AD vs NC (based on left hippocampal volume)* Accuracy: 94.8%
Zhang et al.[23]	T1 weighted	3D CNN	*AD vs NC:* - Accuracy: 97.35% *pMCI vs sMCI:* - Accuracy: 78.7% *NC vs pMCI:* - Accuracy: 87.8%
Feng et al.[24]	MRI and PET	3D CNN	*AD vs NC:* - Acc: 94.8% *pMCI vs NC:* - Acc: 86.3% *sMCI vs NC:* - Acc: 65.3%
Bi et al.[25]	rs-fMRI	ELM and RNN	On recur-ELM *Using 3-class:*- Accuracy: 0.847 ± 0.038CI *Using NC-AD:*- Accuracy: 0.913 ± 0.011CI *Using NC-MCI:*- Accuracy:0.805 ± 0.095CI *Using MCI-AD:*- Accuracy: 0.824 ± 0.039CI
Nguyen et al.[26]	MRI, CSF and PET	minimal-RNN	mAUC: - 0.944 $\pm$ 0.014
Ebrahimi and Luo[27]	3D MRI	LSTM	Accuracy: 96.88%
Basheera and Ram [28]	T1 and T2 weighted MRI	CNN	*AD vs NC:* - Acc:92% *MCI vs NC:* - Acc: 88.2% *AD vs MCI:* - Acc: 91.6%

This research [29] examines binary classification using FDOPA PET scan textural features. They used 443 and 100 PET/CT scans from separate systems for feature selection and model testing. They constructed logistic regression models using LASSO regularization, incorporating a set of 43 biomarkers that encompass 32 textural characteristics. The AUROC of the model improves by 63.91 using textural features. With GLCM Correlation as the most independent variable, the model has great sensitivity and specificity. Textural traits may help diagnose parkinsonian disorders.

In [30], a deep learning framework is introduced for Parkinson's disease diagnosis by leveraging the learning of sMRI T2 slice features. This framework incorporates a DCNN, an adaptive weighted attention algorithm, a dropout layer, and a softMax layer to achieve precise classification results and capture a wide range of feature information. The most notable achievement of this proposed approach was an impressive accuracy rate of 92%. Additionally, it exhibited a sensitivity of 94%, an F1 score of 95%, and specificity of 90%, and all of which were instrumental in effectively distinguishing between individuals with PD and healthy controls.

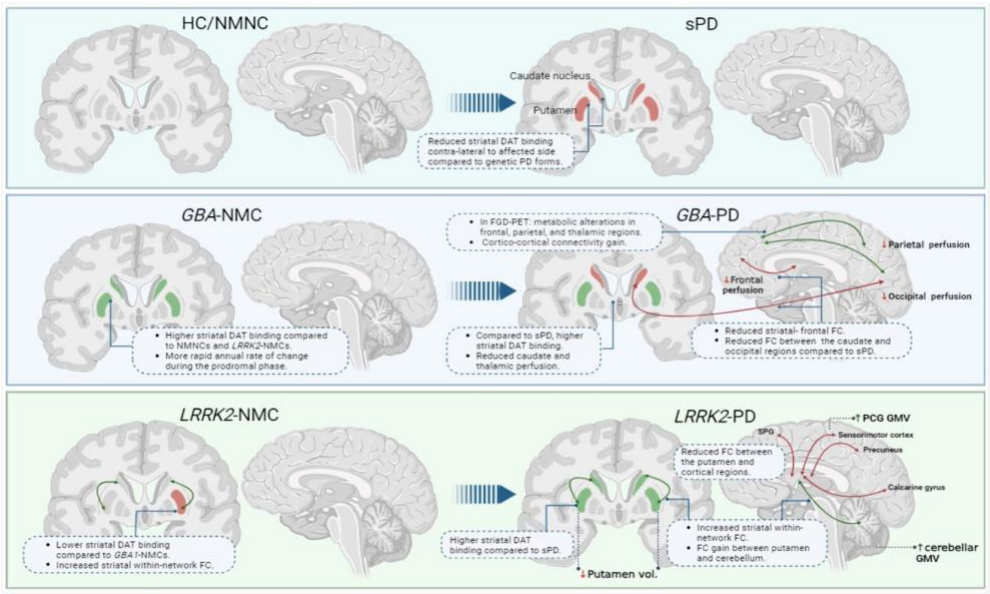

Figure 5. Visual representation summarizing imaging observations extracted from both nuclear imaging and MRI studies. Abbreviations: NMC = non-manifesting carrier, PD = Parkinson's disease, FC = functional connectivity, HC = healthy control, sPD = sporadic PD, , NMNC = non-manifesting non-carrier, vol = volume, DAT = dopamine transporter, GMV = gray matter volume [31].

In [32], the primary goal was to create and assess a robust and interpretable DL architecture for classifying PD using a dataset comprising 2,041 T1-weighted MRI scans from 13 different studies. The preprocessing steps involved skull stripping, resampling, bias field correction, and registration to the MNI PD25 atlas. A state-of-the-art CNN was trained using Jacobian maps and clinical parameters. To enhance interpretability, saliency maps were generated to highlight the brain regions contributing significantly to the classification process. The CNN model demonstrated strong performance, achieving an accuracy of 79.3%, precision, specificity, sensitivity and an AUC-ROC score of 80.2%, 81.3%, 77.7%, and 0.87 respectively when evaluated on the test dataset. Other noteworthy attempts [33–37]for the PD detection is supported in the literature mentioned in Table 3.

Table 3. DL approaches for the classification of Parkinson's disease.

Author	Image Modality	Models Employed	Results
Z. Maalej et al [38]	PET	LSTM	Accuracy: 84%
B Battula et al [39]	MRI	ResNeXt	Accuracy: 100%.
T.M. Tassew [40]	DaTScan and T2-weighted MRI	YOLOv7x and UNet	*Using YOLOv7x* *for DaTScan images* mAP_0.5:0.95 of 70.39 % *for MRI images* mAP_0.5:0.95 of 64.16 %
I D. Apostolopoulos [41]	MRI	AFF-VGG19	Accuracy: 0.9565
S. Sivaranjini [42]	MRI	AlexNet	Accuracy: 88.9%
M Thakur et al [43]	single-photon emission computerized tomography (SPECT) images	DenseNet-121	Accuracy: 99.2%; AUC-ROC: 99% Sensitivity: 99.2%; specificity: 99.4% F1-score: 99.1%

4.2 Cancer Diagnosis

Deep learning has emerged as a powerful technique for tackling the challenges of lung cancer and breast cancer. In lung cancer, deep learning models excel at detecting nodules in medical images like CT scans, aiding in early diagnosis. Similarly, in breast cancer, these models analyze mammograms, MRIs, ultrasound, and histopathology images to identify abnormalities, estimate risk, and guide personalized treatment plans. These models aid in identifying subtle patterns and anomalies that might be missed by traditional methods. Despite these advancements, challenges such as data availability, interpretability, and regulatory approval remain important considerations for real-world clinical implementation. This section encompasses a discussion on diverse DL techniques employed for the detection of breast cancer and lung cancer.

Lung cancer

This work [44] proposed a comprehensive system to detect lung cancer (LC) in CT scan images. This system comprises of two core components: firstly, a segmentation module built upon the UNETR network, and secondly, a classification module employing a self-supervised network to categorize the segmented output into benign or malignant. By leveraging 3D-input CT scan data, their model emerges as a robust tool for timely lung cancer diagnosis. Through rigorous experimentation on the Decathlon dataset, they achieved 97.83% of accuracy for segmentation and 98.77% of accuracy for classification. Figure 6 shows various imaging findings for chest CT scans. Other research attempts for the lung cancer detection are listed in Table 4.

A novel deep learning framework called LCD-CapsNet has been introduced in [45], which combines the capabilities of a CNN and a Capsule Neural Network (CapsNet). This fusion leverages the strengths of both networks to efficiently handle extensive data and achieve spatial invariance. The primary objective of this framework is to classify the lung cancer using CT scans, specifically utilizing the Lung Image Database Consortium (LIDC) datasets for evaluation. Remarkably, this deep learning model outperforms CapsNet in various metrics, boasting an average precision, a recall, an F1-score, a specificity, an AUC of 95%, 94.5%, 94.5%, 99.07%, 0.989, and an accuracy rate of 94% for distinguishing between benign and malignant data.

The study in [46], aimed to evaluate the effectiveness of the Swin Transformer in the tasks of LC classification and segmentation. The pre-trained Swin-B model achieved an impressive top-1 accuracy of 82.26% in classification, which outperformed ViT by a margin of 2.529%. Furthermore, the Swin-S model demonstrated superior segmentation performance compared to alternative methods, as indicated by its mean Intersection over Union (mIoU). These findings highlight the efficacy of pre-training as a valuable strategy to enhance the precision of the Swin Transformer model specifically for these tasks.

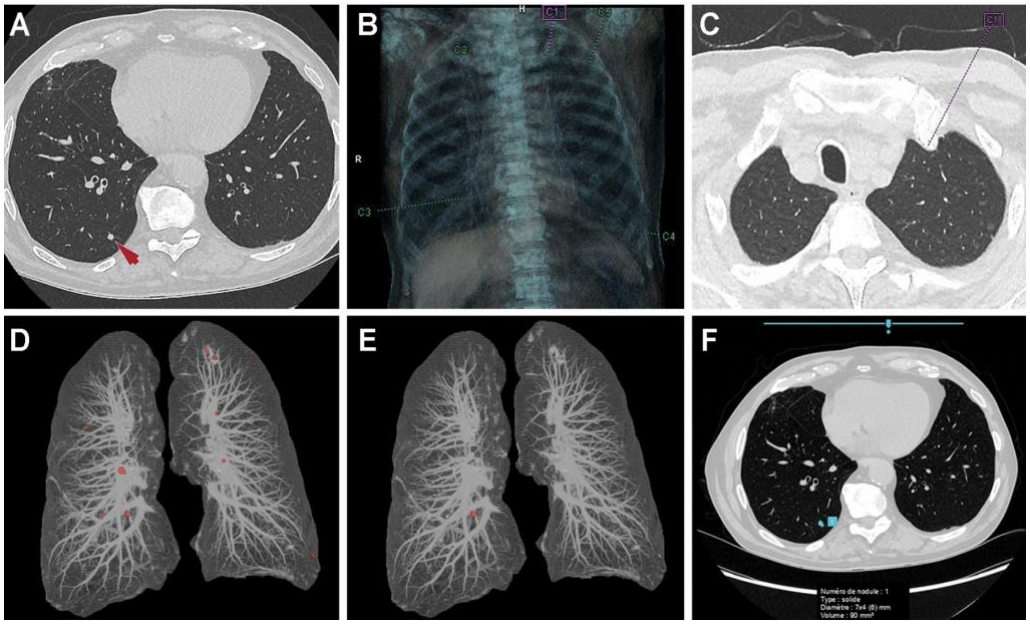

Figure 6. (A) a chest CT image in axial view displays a 7 × 4 mm solid nodule (indicated by an arrow) situated in the lower right lobe. (B) and (C): Utilizing a classical machine learning-based computer-aided detection (CADe) approach, the nodule is accurately identified, accompanied by four false positives (one false positive is marked in C). D and E: Employing another CADe tool rooted in classical machine learning, the nodule is also correctly detected. Adjusting the sensitivity for 3-mm nodule detection introduces multiple false positives (D), while setting the threshold at 6-mm eliminates false positives (E). (F): A CADe tool built on deep learning principles successfully recognizes the nodule without any false positives [47].

In [48], a novel, comprehensive, and efficient deep learning technique called E2EFP-MIL (end-to-end feature pyramid deep multi-instance learning model) was introduced for weakly supervised learning. This approach incorporates three key modules: an iterative sampling module, a trainable feature pyramid module, and a resilient feature aggregation module. E2EFP-MIL adopts an end-to-end learning strategy, enabling the automatic extraction of generalized morphological features, which in turn facilitates the identification of unique histomorphological patterns. The model is trained on a dataset comprising 1007 whole slide images (WSIs) of LC from TCGA and achieves impressive AUC values ranging from 0.95 to 0.97 on test sets. When validated on diverse real-world cohorts, encompassing approximately 1600 WSIs from both the United States and China, E2EFP-MIL consistently demonstrates robust performance, achieving AUCs between 0.94 and 0.97, even with a limited training dataset of 100 to 200 images. This performance surpasses existing MIL-based methods, and notably, E2EFP-MIL combines high accuracy with modest hardware requirements, underlining its potential for clinical applications.

Table 4. DL models for the classification and detection of lung cancer.

Author	Image Modality	Models Employed	Results
K.Barbouchi [49]	PET/CT	Transformer based DNN	Intersection over union (IOU): 0.8 *For classification of T-stage:-* accuracy = 0.97 *For histologic subtypes:-* accuracy = 0.94
V. Bishnoi [50]	Histopathological images	*Color-based Dilated CNN*	Across the Cancer Genome Atlas dataset, the Clinical Proteomic Tumor Analysis Consortium cohorts, and the LC25000 dataset Accuracy: 0.97 to 0.99; while precision, recall, and F1 scores consistently reached values between 0.97 and 0.98. AUC: 0.970 to 0.984; kappa score : 0.986.
B.R.Pandit [51]	CT images	CNN	Classification accuracy : 99.5% - 98.9%
I Naseer [52]	CT scans	For segmentation: modified U-Net For classification: modified AlexNet + support vector machine	Accuracy: 97.98%, sensitivity :98.84%, specificity: 97.47%, precision 97.53%, F1- score : 97.70%
M A Balci [53]	CT scans	U-shape convolutional neural networks	Accuracy : 92.84%
S Nigudgi [54]	CT scans	For feature extraction: AlexNet, VGG and GoogleNet For classification: SVM	Accuracy : 97%

Breast cancer

In [55], a novel DL model to classify the breast cancer was introduced. This model draws inspiration from GoogLeNet and incorporates elements of residual blocks. By integrating adopted granular computing, shortcut connections, two trainable activation functions (in contrast to traditional activation functions), and an attention mechanism, the model demonstrates the potential to significantly improve diagnostic accuracy. Remarkably, the model achieves an accuracy rate of 93% when applied to ultrasound images and an even higher accuracy of 95% when dealing with breast histopathology images.

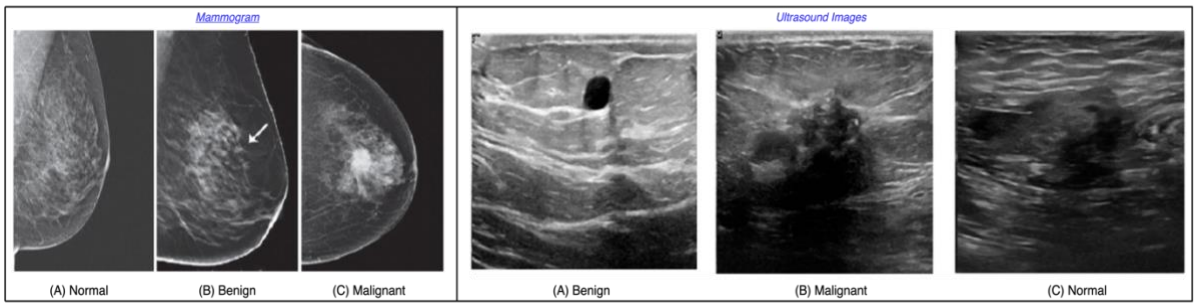

Figure 7. Image samples of Normal, benign and malignant of breast mammograms and ultrasound [56].

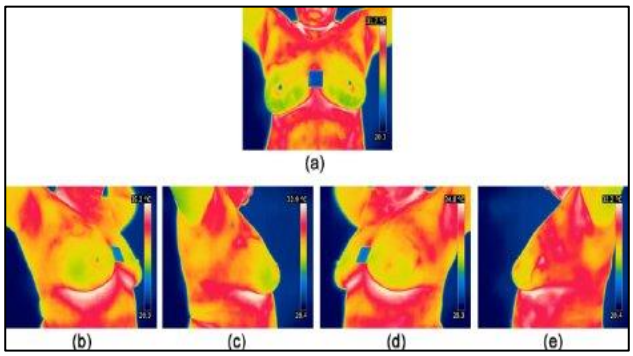

Figure 8. Thermal image samples with Positions (a) Front, (b) Right Lateral 45°, (c) Right Lateral 90°, (d) Left Lateral 45°, (e) and Left Lateral 90° [57].

Table 5. DL models for the classification and detection of breast cancer.

Author	Image Modality	Models Employed	Results
A Sahu et al [58]	Mammogram Ultrasound	ShuffleNet-ResNet	*On mini-DDSM dataset:* 99.17% and 98.00% of accuracies in detecting abnormalities and malignancy. *On BUSI dataset:* 96.52% and 93.18% of accuracies in detecting abnormalities and malignancy *On BUS2 dataset:* 98.13% of accuracy in malignancy detection
K Atrey et al [59]	Mammogram Ultrasound	CNN + LSTM	*On mammogram* dataset :-Accuracy : 97.16% *On ultrasound dataset* :-Accuracy : 98.84%
F Prinzi et al[60]	Mammogram	YoloV5	mAP: 0.838 ± 0.042; recall: 0.722 ± 0.096; precision: 0.917 ± 0.077,
J.Zuluaga Gomez et al [61]	Thermal images	CNN	Accuracy: 92% F1-score: 92%
S S Boudouh et al [62]	Mammogram	Xception, InceptionV3, ResNet101V2, ResNet50V2, ALexNet, VGG16, and VGG19	*Using ResNet50V2* Accuracy: 99.9%, *Using InceptionV3* Accuracy: 99.54%
T Liao [63]	Mammogram	DenseNet convolution neural network	Specificity (0.909 vs. 0.835, 0.790, X^2=8.21 and 17.22, p ＜0.05) and precision (0.872 vs. 0.763, 0.726, X^2=9.23 and 5.22, p＜0.05)
S Civilibal [64]	Thermal images	Mask R-CNN + Transfer learning	Accuracy: 97.1%
S Gupta [65]	Ultrasound	Modified ResNet50	Accuracy: 97.8%; recall: 97.68%; precision: 99.21%; F1-score: 98.44%.

The research [66] introduced a deep learning CNN, which effectively distinguishes between benign and malignant tumor categories. The model's effectiveness is assessed using key metrics, including sensitivity, precision, accuracy, F1-score, and the AUC. A five-fold cross-validation approach was used for evaluation. The findings affirm the effectiveness of the proposed model, showcasing a robust accuracy of 98.2% in successfully identifying breast cancer anomalies.

In [67], a hybrid model was created, combining a CNN with a LSTM-RNN for the purpose of classifying four different subtypes of benign and malignant breast cancer. This model underwent evaluation using the BreakHis image dataset, which consists of 2480 benign and 5429 malignant cases. During experimentation, it was determined that the Adam optimizer yielded the best results, achieving minimum model loss and maximum accuracy. This model attained an exceptional 99% of accuracy for binary classification, effectively distinguishing between benign and malignant cases. Additionally, for the more challenging multi-class classification involving both cancer types, the model achieved an accuracy rate of 92.5%. Figures 7 and 8 provide visual representations of various imaging modalities used in breast cancer detection.

In [68], a study was conducted where they introduced an ensemble DL system designed to detect breast cancer. This system leverages Suspected Nodule Regions (SNRs) extracted using an optimal dynamic thresholding method. The ensemble itself comprises four CNNs along with a binary SVM. When tested on ROI images, this system exhibited outstanding performance, achieving a remarkable 94% of accuracy for the classification of malignant and benign classes and an even higher 95% of accuracy for the classification of malignant and benign mass nodules. Additionally, Table 5 provides an overview of the various applications of deep learning models in the context of breast cancer detection.

Ophthalmology

Deep learning is being increasingly applied in the field of ophthalmology for various detection tasks, ranging from disease identification to anomaly detection. This innovative approach leverages large datasets and complex neural networks to improve the efficiency of diagnosing ophthalmic conditions. By training deep neural networks on diverse ophthalmic data, including retinal images, OCT scans, and visual field data, significant advancements have been made in automating the detection of conditions like diabetic retinopathy, glaucoma, age-related macular degeneration, etc. Figure 9 and Figure 10 depicts the OCT scans and fundus images of healthy subjects and glaucoma patients. Table 6 lists other notable contributions for the detection of various eye diseases.

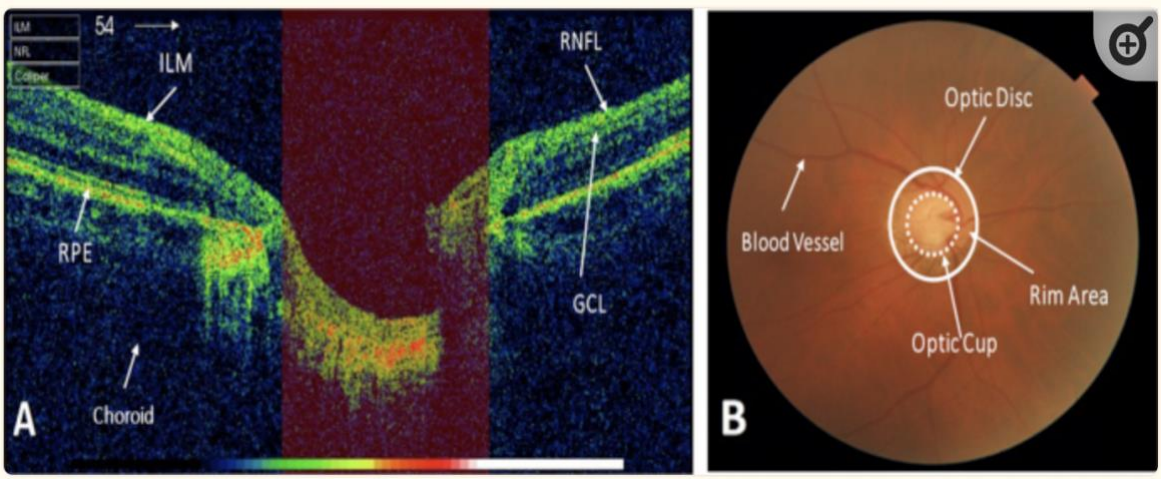

Figure 9. Images of the left ocular organ. A) An OCT image illustrating the retinal strata utilized in the identification of Glaucoma: The innermost ILM layer, followed by the RNFL layer, Ganglion cell layer, and concluding with the RPE layer. B) A Fundus image displaying the optic disc, optic cup, the surrounding rim area, and the vasculature. [69].

In study [70], an assessment was conducted for the evaluation of an automated artificial intelligence algorithm known as EyeArt v2.1. The algorithm's objective was to triage retinal images from the English Diabetic Eye Screening Programme (DESP) into two categories: test-positive and test-negative. The sensitivity of EyeArt for detecting referable retinopathy was determined to be 95.7%, with a 95% confidence interval ranging from 94.8% to 96.5%. This sensitivity included values of 98.3% for mild-to-moderate non-proliferative retinopathy with referable maculopathy, 100% for moderate-to-severe non-proliferative retinopathy, and 100% for proliferative disease. Regarding EyeArt's alignment with human grading, which represents the absence of retinopathy (specificity), it was observed in 68% of cases, with a range between 67% to 69%. However, when combined with non-referable retinopathy, the specificity decreased to 54.0%, with a range of 53.4% to 54.5%.

In the research [71], the study delved into the application of ultrawide-field fundus images in combination with a DCNN to identify treatment-naive proliferative diabetic retinopathy (PDR). Their approach involved training the DCNN using a dataset consisting of 378 photographic images, comprising 132 cases of PDR and 246 cases of non-PDR. The subsequent evaluation included assessing metrics like AUC, sensitivity, and specificity. The model obtained a specificity of 97.2%, sensitivity of 94.7% and an AUC value of 0.969.

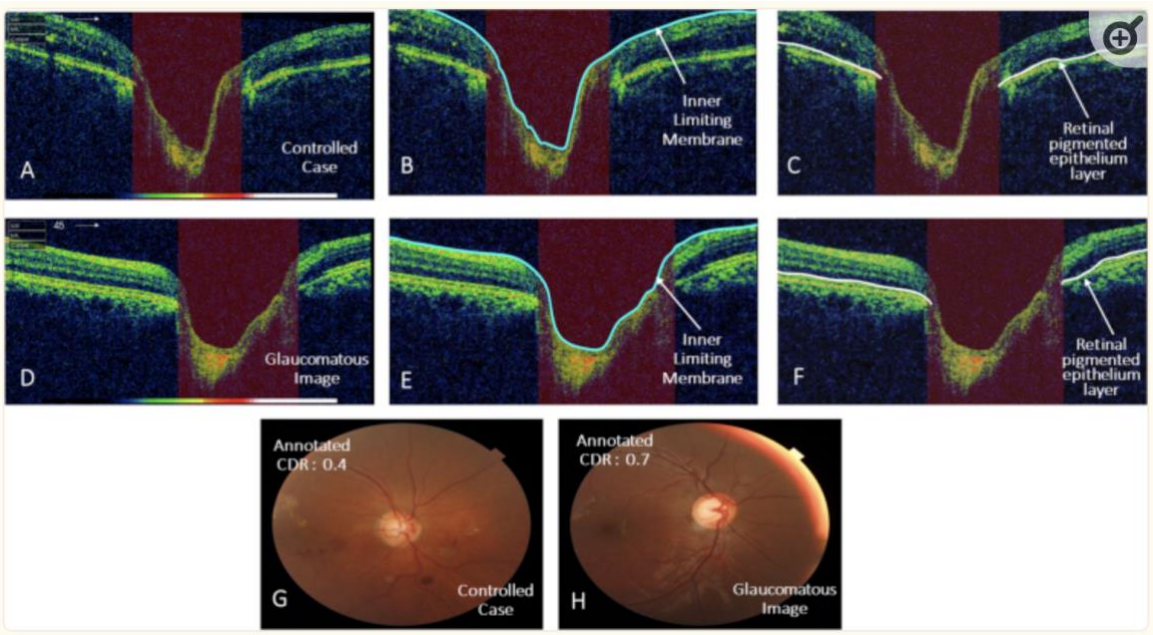

Figure 10. OCT and Fundus visuals representing individuals with controlled and those with glaucoma; The images of the controlled subject are presented in (A) and (G). The delineation of the corresponding ILM and RPE layers can be observed in (B) and (C). Depictions of OCT and Fundus imagery for subjects with glaucoma can be found in (D) and (H), while manually extracted ILM and RPE layers are accentuated in (E) and (F) [69].

Table 6. applications of various deep learning architectures in the ophthalmology disease detection.

Author	Image Modality	Models Employed	Results
J ko et al [72]	spectral domain optical coherence tomography (SD-OCT) scans	(CNN-LSTM)	Accuracy: 94.2%
YB Chou et al [73]	Color fundus photographs OCT scans	novel bi-modal DL model	Accuracy: 80.76%; Sensitivity: 83.67% Specificity: 84.72; AUC-ROC: 88.57%
J Loo et al [74]	OCT scans	CNN	Sensitivity: 0.94; Specificity: 0.80 average Dice similarity coefficient: 0.94±0.07
H Stegmann et al [75]	OCT scans	CNN	*For the DSA* Sensitivity: 96.36%; Specificity: 99.98% Jaccard index: 93.24% *For the LSA* Sensitivity:96.43%; Specificity 99.86% Jaccard index:93.16%
H Abdelmotaal et al [76]	Color-coded Scheimpflug images	CNN	*For the training set* Accuracy:0.983 *For the test set* Accuracy: 0.958
H K Yang [77]	Fundus photographs	ResNet 50	Sensitivity: 93.4% Specificity: 81.8%

In [78], the objective was to develop diagnostic technology capable of automatically grading the severity of diabetic retinopathy using both ultra-widefield fluorescein angiography (UWFA) and the Early Treatment Diabetic Retinopathy Study (ETDRS) 7-standard field images. A cross-sectional study was conducted using a dataset of 280 diabetic patients and 119 individuals without diabetes for training and testing an artificial intelligence model. The results demonstrated an accuracy of 88.50% when using original UWFA images and 73.68% accuracy when using simulated 7-SF images. Notably, a simple linear regression function highlighted a significant relationship between the ischemic index and leakage index and the severity of diabetic retinopathy. Furthermore, by optimizing the cycle generative adversarial network and convolutional neural network model classifier, the accuracy of diabetic retinopathy grading was improved, with slightly better results obtained when using UWFA images.

In [79], the research focused on assessing the influence of a multi-input deep learning strategy for analyzing optical coherence tomography (OCT), OCT angiography (OCT-A), and color fundus photographs. The aim was to improve the accuracy of a CNN in the diagnosis of intermediate dry age-related macular degeneration (AMD). The research involved 75 participants categorized into three groups. Training the CNN on multiple image modalities simultaneously resulted in increased accuracy: 94% for OCT alone, 91% for OCT-A, and 96% when combining multiple modalities for AMD diagnosis. The study demonstrates the potential of deep learning combined with multimodal image analysis for achieving superior diagnostic accuracy.

5. Conclusion

Recent advances in machine learning, particularly in the domain of DL, have triggered substantial progress in the detection, categorization, and quantification of inherent patterns within medical images. A significant breakthrough lies in the capacity to leverage hierarchical feature representations acquired solely from data, eliminating the necessity for manually crafted features reliant on domain-specific expertise. Deep learning algorithms consistently demonstrate enhanced performance across a broad spectrum of medical applications.

In the realm of medical imaging, the emergence of DL has ushered in a novel era characterized by remarkable advancements in the areas of disease detection. This chapter explores the captivating array of deep learning applications across various disciplines like neurology, cancer identification, ophthalmology, each examined through the lens of medical imaging. The transformative power of deep learning algorithms is fully realized as they navigate the intricate landscapes of medical imaging, revealing concealed intricacies and deviations. Their exceptional capability deciphers the complexities of neurodegenerative disorders such as Parkinson's and Alzheimer's, and in the precision of detecting cancers like those affecting the lungs and breasts. Ophthalmology also benefits significantly from these intelligent systems, fundamentally altering the trajectory of medical practice. Overall, deep learning has revolutionized medical imaging and significantly enhanced disease diagnosis and patient care.

References

[1] LeCun Y, Bengio Y, Hinton G. Deep learning. Nature 2015;521:436–44. https://doi.org/10.1038/nature14539.

[2] Dahl GE, Dong Yu, Li Deng, Acero A. Context-Dependent Pre-Trained Deep Neural Networks for Large-Vocabulary Speech Recognition. IEEE Trans Audio Speech Lang Process 2012;20:30–42. https://doi.org/10.1109/TASL.2011.2134090.

[3] Krizhevsky A, Sutskever I, Hinton GE. ImageNet Classification with Deep Convolutional Neural Networks. In: Pereira F, Burges CJ, Bottou L, Weinberger KQ, editors. Adv Neural Inf Process Syst, vol. 25, Curran Associates, Inc.; 2012.

[4] Shen D, Wu G, Suk H-I. Deep Learning in Medical Image Analysis. Annu Rev Biomed Eng 2017;19:221–48. https://doi.org/10.1146/annurev-bioeng-071516-044442.

[5] Pawlowski N, Ktena SI, Lee MCH, Kainz B, Rueckert D, Glocker B, et al. DLTK: State of the Art Reference Implementations for Deep Learning on Medical Images 2017.

[6] Lakhani P, Gray DL, Pett CR, Nagy P, Shih G. Hello World Deep Learning in Medical Imaging. J Digit Imaging 2018;31:283–9. https://doi.org/10.1007/s10278-018-0079-6.

[7] Kim J, Hong J, Park H. Prospects of deep learning for medical imaging. Precision and Future Medicine 2018;2:37–52. https://doi.org/10.23838/pfm.2018.00030.

[8] Lu L, Zheng Y, Carneiro G, Yang L, editors. Deep Learning and Convolutional Neural Networks for Medical Image Computing. Cham: Springer International Publishing; 2017. https://doi.org/10.1007/978-3-319-42999-1.

[9] Ketkar N, Moolayil J. Deep Learning with Python. Berkeley, CA: Apress; 2021. https://doi.org/10.1007/978-1-4842-5364-9.

[10] Lecun Y, Bottou L, Bengio Y, Haffner P. Gradient-based learning applied to document recognition. Proceedings of the IEEE 1998;86:2278–324. https://doi.org/10.1109/5.726791.

[11] HUBEL DH, WIESEL TN. Receptive fields, binocular interaction and functional architecture in the cat's visual cortex. J Physiol 1962;160:106–54. https://doi.org/10.1113/jphysiol.1962.sp006837.

[12] WILLIAMS RJ, ZIPSER D. Experimental Analysis of the Real-time Recurrent Learning Algorithm. Conn Sci 1989;1:87–111. https://doi.org/10.1080/09540098908915631.

[13] Hinton GE, Salakhutdinov RR. Reducing the Dimensionality of Data with Neural Networks. Science (1979) 2006;313:504–7. https://doi.org/10.1126/science.1127647.

[14] Zheng B, Gao A, Huang X, Li Y, Liang D, Long X. A modified 3D EfficientNet for the classification of Alzheimer's disease using structural magnetic resonance images. IET Image Process 2023;17:77–87. https://doi.org/10.1049/ipr2.12618.

[15] Bamber SS, Vishvakarma T. Medical image classification for Alzheimer's using a deep learning approach. Journal of Engineering and Applied Science 2023;70. https://doi.org/10.1186/s44147-023-00211-x.

[16] Janghel RR, Rathore YK. Deep Convolution Neural Network Based System for Early Diagnosis of Alzheimer's Disease. IRBM 2021;42:258–67. https://doi.org/10.1016/j.irbm.2020.06.006.

[17] Johnson KA, Fox NC, Sperling RA, Klunk WE. Brain Imaging in Alzheimer Disease. Cold Spring Harb Perspect Med 2012;2:a006213–a006213. https://doi.org/10.1101/cshperspect.a006213.

[18] Zhou Z, Yu L, Tian S, Xiao G. Diagnosis of Alzheimer's disease using 2D dynamic magnetic resonance imaging. J Ambient Intell Humaniz Comput 2023;14:10153–63. https://doi.org/10.1007/s12652-021-03678-9.

[19] Park HY, Shim WH, Suh CH, Heo H, Oh HW, Kim J, et al. Development and validation of an automatic classification algorithm for the diagnosis of Alzheimer's disease using a high-performance interpretable deep learning network. Eur Radiol 2023. https://doi.org/10.1007/s00330-023-09708-8.

[20] Wang Y, He N, Zhang C, Zhang Y, Wang C, Huang P, et al. An automatic interpretable deep learning pipeline for accurate Parkinson's disease diagnosis using quantitative susceptibility mapping and <scp>T1-weighted images</scp>. Hum Brain Mapp 2023;44:4426–38. https://doi.org/10.1002/hbm.26399.

[21] Mehmood A, Maqsood M, Bashir M, Shuyuan Y. A Deep Siamese Convolution Neural Network for Multi-Class Classification of Alzheimer Disease. Brain Sci 2020;10:84. https://doi.org/10.3390/brainsci10020084.

[22] Basher A, Kim BC, Lee KH, Jung HY. Volumetric Feature-Based Alzheimer's Disease Diagnosis From sMRI Data Using a Convolutional Neural Network and a Deep Neural Network. IEEE Access 2021;9:29870–82. https://doi.org/10.1109/ACCESS.2021.3059658.

[23] Zhang J, Zheng B, Gao A, Feng X, Liang D, Long X. A 3D densely connected convolution neural network with connection-wise attention mechanism for Alzheimer's disease classification. Magn Reson Imaging 2021;78:119–26. https://doi.org/10.1016/j.mri.2021.02.001.

[24] Feng C, Elazab A, Yang P, Wang T, Zhou F, Hu H, et al. Deep Learning Framework for Alzheimer's Disease Diagnosis via 3D-CNN and FSBi-LSTM. IEEE Access 2019;7:63605–18. https://doi.org/10.1109/ACCESS.2019.2913847.

[25] Bi X, Zhao X, Huang H, Chen D, Ma Y. Functional Brain Network Classification for Alzheimer's Disease Detection with Deep Features and Extreme Learning Machine. Cognit Comput 2020;12:513–27. https://doi.org/10.1007/s12559-019-09688-2.

[26] Nguyen M, He T, An L, Alexander DC, Feng J, Yeo BTT. Predicting Alzheimer's disease progression using deep recurrent neural networks. Neuroimage 2020;222:117203. https://doi.org/10.1016/j.neuroimage.2020.117203.

[27] Ebrahimi A, Luo S, Chiong R. Deep sequence modelling for Alzheimer's disease detection using MRI. Comput Biol Med 2021;134:104537. https://doi.org/10.1016/j.compbiomed.2021.104537.

[28] Basheera S, Ram MSS. Deep learning based Alzheimer's disease early diagnosis using T2w segmented gray matter <scp>MRI</scp>. Int J Imaging Syst Technol 2021;31:1692–710. https://doi.org/10.1002/ima.22553.

[29] Comte V, Schmutz H, Chardin D, Orlhac F, Darcourt J, Humbert O. Development and validation of a radiomic model for the diagnosis of dopaminergic denervation on [18F]FDOPA PET/CT. Eur J Nucl Med Mol Imaging 2022;49:3787–96. https://doi.org/10.1007/s00259-022-05816-7.

[30] Cui X, Chen N, Zhao C, Li J, Zheng X, Liu C, et al. An adaptive weighted attention-enhanced deep convolutional neural network for classification of MRI images of Parkinson's disease. J Neurosci Methods 2023;394:109884. https://doi.org/10.1016/j.jneumeth.2023.109884.

[31] Droby A, Thaler A, Mirelman A. Imaging Markers in Genetic Forms of Parkinson's Disease. Brain Sci 2023;13:1212. https://doi.org/10.3390/brainsci13081212.

[32] Camacho M, Wilms M, Mouches P, Almgren H, Souza R, Camicioli R, et al. Explainable classification of Parkinson's disease using deep learning trained on a large multi-center database of T1-weighted MRI datasets. Neuroimage Clin 2023;38:103405. https://doi.org/10.1016/j.nicl.2023.103405.

[33] Khanna K, Gambhir S, Gambhir M. Comparative analysis of machine learning techniques for Parkinson's detection: A review. Multimed Tools Appl 2023. https://doi.org/10.1007/s11042-023-15414-w.

[34] Nissar I, Rizvi D, Masood S, Mir A. Voice-Based Detection of Parkinson's Disease through Ensemble Machine Learning Approach: A Performance Study. EAI Endorsed Trans Pervasive Health Technol 2019;5:162806. https://doi.org/10.4108/eai.13-7-2018.162806.

[35] Nissar I, Mir WA, Izharuddin, Shaikh TA. Machine Learning Approaches for Detection and Diagnosis of Parkinson's Disease - A Review. 2021 7th International Conference on Advanced Computing and Communication Systems (ICACCS), IEEE; 2021, p. 898–905. https://doi.org/10.1109/ICACCS51430.2021.9441885.

[36] Mir WA, Nissar I, Izharuddin, Rizvi DR, Masood S, Hussain A. Deep Learning-based model for the detection of Parkinson's disease using voice data. 2022 First International Conference on Artificial Intelligence Trends and Pattern Recognition (ICAITPR), IEEE; 2022, p. 1–6. https://doi.org/10.1109/ICAITPR51569.2022.9844185.

[37] Ahmad Mir W, Izharuddin, Nissar I. Contribution of Application of Deep Learning Approaches on Biomedical Data in the Diagnosis of Neurological Disorders: A Review on Recent Findings, 2020, p. 87–97. https://doi.org/10.1007/978-981-15-3666-3_8.

[38] Maalej Z, Rejab F Ben, Nouira K. Deep Learning for Parkinson's Disease Severity Stage Prediction Using a New Dataset, 2023, p. 110–23. https://doi.org/10.1007/978-3-031-34960-7_8.

[39] Balnarsaiah B, Nayak BA, Sujeetha GS, Babu BS, Vallabhaneni RB. Parkinson's disease detection using modified ResNeXt deep learning model from brain MRI images. Soft Comput 2023;27:11905–14. https://doi.org/10.1007/s00500-023-08535-9.

[40] Tassew TM, Xuan N, Chai B. PDDS: A software for the early diagnosis of Parkinson's disease from MRI and DaT scan images using detection and segmentation algorithms. Biomed Signal Process Control 2023;86:105140. https://doi.org/10.1016/j.bspc.2023.105140.

[41] Apostolopoulos ID, Aznaouridis S, Tzani M. An Attention-Based Deep Convolutional Neural Network for Brain Tumor and Disorder Classification and Grading in Magnetic Resonance Imaging. Information 2023;14:174. https://doi.org/10.3390/info14030174.

[42] Sivaranjini S, Sujatha CM. Deep learning based diagnosis of Parkinson's disease using convolutional neural network. Multimed Tools Appl 2020;79:15467–79. https://doi.org/10.1007/s11042-019-7469-8.

[43] Thakur M, Kuresan H, Dhanalakshmi S, Lai KW, Wu X. Soft Attention Based DenseNet Model for Parkinson's Disease Classification Using SPECT Images. Front Aging Neurosci 2022;14. https://doi.org/10.3389/fnagi.2022.908143.

[44] Said Y, Alsheikhy AA, Shawly T, Lahza H. Medical Images Segmentation for Lung Cancer Diagnosis Based on Deep Learning Architectures. Diagnostics 2023;13:546. https://doi.org/10.3390/diagnostics13030546.

[45] A.R. B, R.S. VK, S.S. K. LCD-Capsule Network for the Detection and Classification of Lung Cancer on Computed Tomography Images. Multimed Tools Appl 2023. https://doi.org/10.1007/s11042-023-14893-1.

[46] Sun R, Pang Y, Li W. Efficient Lung Cancer Image Classification and Segmentation Algorithm Based on an Improved Swin Transformer. Electronics (Basel) 2023;12:1024. https://doi.org/10.3390/electronics12041024.

[47] Chassagnon G, De Margerie-Mellon C, Vakalopoulou M, Marini R, Hoang-Thi T-N, Revel M-P, et al. Artificial intelligence in lung cancer: current applications and perspectives. Jpn J Radiol 2022. https://doi.org/10.1007/s11604-022-01359-x.

[48] Cao L, Wang J, Zhang Y, Rong Z, Wang M, Wang L, et al. E2EFP-MIL: End-to-end and high-generalizability weakly supervised deep convolutional network for lung cancer classification from whole slide image. Med Image Anal 2023;88:102837. https://doi.org/10.1016/j.media.2023.102837.

[49] Barbouchi K, El Hamdi D, Elouedi I, Aïcha T Ben, Echi AK, Slim I. A transformer-based deep neural network for detection and classification of lung cancer via <scp>PET</scp> / <scp>CT</scp> images. Int J Imaging Syst Technol 2023;33:1383–95. https://doi.org/10.1002/ima.22858.

[50] Bishnoi V, Goel N. A color-based deep-learning approach for tissue slide lung cancer classification. Biomed Signal Process Control 2023;86:105151. https://doi.org/10.1016/j.bspc.2023.105151.

[51] Pandit BR, Alsadoon A, Prasad PWC, Al Aloussi S, Rashid TA, Alsadoon OH, et al. Deep learning neural network for lung cancer classification: enhanced optimization function. Multimed Tools Appl 2023;82:6605–24. https://doi.org/10.1007/s11042-022-13566-9.

[52] Naseer I, Akram S, Masood T, Rashid M, Jaffar A. Lung Cancer Classification Using Modified U-Net Based Lobe Segmentation and Nodule Detection. IEEE Access 2023;11:60279–91. https://doi.org/10.1109/ACCESS.2023.3285821.

[53] Balcı MA, Batrancea LM, Akgüller Ö, Nichita A. A Series-Based Deep Learning Approach to Lung Nodule Image Classification. Cancers (Basel) 2023;15:843. https://doi.org/10.3390/cancers15030843.

[54] Nigudgi S, Bhyri C. Lung cancer CT image classification using hybrid-SVM transfer learning approach. Soft Comput 2023;27:9845–59. https://doi.org/10.1007/s00500-023-08498-x.

[55] Zakareya S, Izadkhah H, Karimpour J. A New Deep-Learning-Based Model for Breast Cancer Diagnosis from Medical Images. Diagnostics 2023;13:1944. https://doi.org/10.3390/diagnostics13111944.

[56] Nissar I, Alam S, Masood S. Recent Trends in Modalities and Deep Learning Methods for Breast Cancer Detection, 2022, p. 416–34. https://doi.org/10.1007/978-3-031-23092-9_33.

[57] Silva LF, Saade DCM, Sequeiros GO, Silva AC, Paiva AC, Bravo RS, et al. A New Database for Breast Research with Infrared Image. J Med Imaging Health Inform 2014;4:92–100. https://doi.org/10.1166/jmihi.2014.1226.

[58] Sahu A, Das PK, Meher S. High accuracy hybrid CNN classifiers for breast cancer detection using mammogram and ultrasound datasets. Biomed Signal Process Control 2023;80:104292. https://doi.org/10.1016/j.bspc.2022.104292.

[59] Atrey K, Singh BK, Bodhey NK, Bilas Pachori R. Mammography and ultrasound based dual modality classification of breast cancer using a hybrid deep learning approach. Biomed Signal Process Control 2023;86:104919. https://doi.org/10.1016/j.bspc.2023.104919.

[60] Prinzi F, Insalaco M, Gaglio S, Vitabile S. Breast Cancer Localization and Classification in Mammograms Using YoloV5, 2023, p. 73–82. https://doi.org/10.1007/978-981-99-3592-5_7.

[61] Zuluaga-Gomez J, Al Masry Z, Benaggoune K, Meraghni S, Zerhouni N. A CNN-based methodology for breast cancer diagnosis using thermal images. Comput Methods Biomech Biomed Eng Imaging Vis 2021;9:131–45. https://doi.org/10.1080/21681163.2020.1824685.

[62] Boudouh SS, Bouakkaz M. Breast cancer: toward an accurate breast tumor detection model in mammography using transfer learning techniques. Multimed Tools Appl 2023. https://doi.org/10.1007/s11042-023-14410-4.

[63] Liao T, Li L, Ouyang R, Lin X, Lai X, Cheng G, et al. Classification of asymmetry in mammography via the DenseNet convolutional neural network. Eur J Radiol Open 2023;11:100502. https://doi.org/10.1016/j.ejro.2023.100502.

[64] Civilibal S, Cevik KK, Bozkurt A. A deep learning approach for automatic detection, segmentation and classification of breast lesions from thermal images. Expert Syst Appl 2023;212:118774. https://doi.org/10.1016/j.eswa.2022.118774.

[65] Gupta S, Agrawal S, Singh SK, Kumar S. A Novel Transfer Learning-Based Model for Ultrasound Breast Cancer Image Classification, 2023, p. 511–23. https://doi.org/10.1007/978-981-19-9819-5_37.

[66] Kaur H. Dense Convolutional Neural Network Based Deep Learning Framework for the Diagnosis of Breast Cancer. Wirel Pers Commun 2023. https://doi.org/10.1007/s11277-023-10678-9.

[67] Srikantamurthy MM, Rallabandi VPS, Dudekula DB, Natarajan S, Park J. Classification of benign and malignant subtypes of breast cancer histopathology imaging using hybrid CNN-LSTM based transfer learning. BMC Med Imaging 2023;23:19. https://doi.org/10.1186/s12880-023-00964-0.

[68] Hekal AA, Moustafa HE-D, Elnakib A. Ensemble deep learning system for early breast cancer detection. Evol Intell 2023;16:1045–54. https://doi.org/10.1007/s12065-022-00719-w.

[69] Raja H, Akram MU, Khawaja SG, Arslan M, Ramzan A, Nazir N. Data on OCT and fundus images for the detection of glaucoma. Data Brief 2020;29:105342. https://doi.org/10.1016/j.dib.2020.105342.
[70] Heydon P, Egan C, Bolter L, Chambers R, Anderson J, Aldington S, et al. Prospective evaluation of an artificial intelligence-enabled algorithm for automated diabetic retinopathy screening of 30 000 patients. British Journal of Ophthalmology 2021;105:723–8. https://doi.org/10.1136/bjophthalmol-2020-316594.
[71] Nagasawa T, Tabuchi H, Masumoto H, Enno H, Niki M, Ohara Z, et al. Accuracy of ultrawide-field fundus ophthalmoscopy-assisted deep learning for detecting treatment-naïve proliferative diabetic retinopathy. Int Ophthalmol 2019;39:2153–9. https://doi.org/10.1007/s10792-019-01074-z.
[72] Ko J, Han J, Yoon J, Park JI, Hwang JS, Han JM, et al. Assessing central serous chorioretinopathy with deep learning and multiple optical coherence tomography images. Sci Rep 2022;12:1831. https://doi.org/10.1038/s41598-022-05051-y.
[73] Chou Y-B, Hsu C-H, Chen W-S, Chen S-J, Hwang D-K, Huang Y-M, et al. Deep learning and ensemble stacking technique for differentiating polypoidal choroidal vasculopathy from neovascular age-related macular degeneration. Sci Rep 2021;11:7130. https://doi.org/10.1038/s41598-021-86526-2.
[74] Loo J, Cai CX, Choong J, Chew EY, Friedlander M, Jaffe GJ, et al. Deep learning-based classification and segmentation of retinal cavitations on optical coherence tomography images of macular telangiectasia type 2. British Journal of Ophthalmology 2022;106:396–402. https://doi.org/10.1136/bjophthalmol-2020-317131.
[75] Stegmann H, Werkmeister RM, Pfister M, Garhöfer G, Schmetterer L, dos Santos VA. Deep learning segmentation for optical coherence tomography measurements of the lower tear meniscus. Biomed Opt Express 2020;11:1539. https://doi.org/10.1364/BOE.386228.
[76] Abdelmotaal H, Mostafa MM, Mostafa ANR, Mohamed AA, Abdelazeem K. Classification of Color-Coded Scheimpflug Camera Corneal Tomography Images Using Deep Learning. Transl Vis Sci Technol 2020;9:30. https://doi.org/10.1167/tvst.9.13.30.
[77] Yang HK, Kim YJ, Sung JY, Kim DH, Kim KG, Hwang J-M. Efficacy for Differentiating Nonglaucomatous Versus Glaucomatous Optic Neuropathy Using Deep Learning Systems. Am J Ophthalmol 2020;216:140–6. https://doi.org/10.1016/j.ajo.2020.03.035.
[78] Wang X, Ji Z, Ma X, Zhang Z, Yi Z, Zheng H, et al. Automated Grading of Diabetic Retinopathy with Ultra-Widefield Fluorescein Angiography and Deep Learning. J Diabetes Res 2021;2021:1–9. https://doi.org/10.1155/2021/2611250.
[79] Vaghefi E, Hill S, Kersten HM, Squirrell D. Multimodal Retinal Image Analysis via Deep Learning for the Diagnosis of Intermediate Dry Age-Related Macular Degeneration: A Feasibility Study. J Ophthalmol 2020;2020:1–7. https://doi.org/10.1155/2020/7493419.